15

Orbital Einstein Cartan Evans (ECE) Theory and Non Einstein Hilbert (EH) Orbits in Astronomy and Cosmology

by

Myron W. Evans,
Alpha Institute for Advanced Study, Civil List Scientist.
(emyrone@aol.com and www.aias.us)

and

Horst Eckardt and K. Pendergast,
Alpha Institute for Advanced Studies (AIAS).
www.aias.us and www.atomicprecision.com

Abstract

It is shown that orbits of all kinds are determined in ECE theory by a well defined ratio of scalar torsion (T) to scalar curvature (R). Non-relativistic and relativistic circular orbits are considered as examples. The orbit of a binary pulsar is reproduced by using the complete theory with T/R as a parameter. It is shown that the precessing ellipse with decreasing orbital radius can be explained in ECE theory without assuming gravitational radiation. The latter is a flawed concept based on the geometrically incorrect Einstein Hilbert (EH) equation. In general orbits cannot be described by the EH theory, but must be described by the geometrically self-consistent ECE theory. Several examples of non-EH orbits are now known, such as binary pulsars and the various Pioneer/Cassini anomalies. These are explained straightforwardly with ECE theory, which also gives a simple explanation for the equivalence principle.

Keywords: Non- EH orbits, ECE theory of orbits, equivalence principle.

15.1 Introduction

It has been shown recently in this series of papers on ECE theory [1–10] that the Einstein Hilbert (EH) field equation is geometrically self-inconsistent because of its neglect of the Cartan torsion. Therefore conclusions based on the EH theory must be discarded and the theory of orbits developed with the geometrically self-consistent ECE theory, a generally covariant unified field theory rigorously based on Cartan geometry [11]. In order to demonstrate the ability of ECE theory to explain orbits straightforwardly, we consider in this paper the various examples of orbits now known not to be describable by the EH theory. Many criticisms of the latter have been made down the years [12] and it is well known to be a deeply flawed theory. It was finally discarded when it was shown using computer algebra [1–10] that the Christoffel connection is incompatible with the fundamental Bianchi identity as given by Cartan [1–11].

In Section 15.2 the general ECE orbital theory is developed in terms of a well defined ratio [1–10] of scalar torsion (denoted T) to scalar curvature (denoted R). This ratio is used as a parameter with which to describe non - EH orbits such as those of binary pulsars, or those observed in the Pioneer/Cassini anomalies. The limit of non-relativistic and relativistic circular orbits is considered as an example. In Section 15.3 the equivalence principle is explained straightforwardly with ECE orbital theory, and in Section 15.4 a perturbatin model of the binary pulsar orbits is developed. Graphical results and discussion are given in section 15.5 for non - EH orbits in binary pulsars and in the solar system, where non-EH orbits are now known from Pioneer and Cassini data. In section 15.6 the Hulse-Taylor binary pulsar is discussed.

15.2 General ECE Orbital Theory

In S.I. units and for a planar orbit, ECE orbital theory is based on the line element:

$$-c^2 d\tau^2 = -\left(1 - \frac{r_S}{r}\right) c^2 dt^2 + \left(1 - \frac{r_S}{r}\right)^{-1} dr^2 + r^2 d\phi^2 \tag{15.1}$$

in spherical polar coordinates. Here [1–10]:

$$r_S = -\frac{T}{R}, \quad |r_S| = \frac{T}{R}, \tag{15.2}$$

where T/R is a parameter determined by the data. An excellent description of the great majority of orbits is found in the limit:

$$r_S \to \frac{2MG}{c^2} \tag{15.3}$$

where G is Newton's constant, and where a mass m is attracted to a gravitating mass M. In the solar system M is the mass of the Sun. In general however Eq. (15.3) does not apply. Examples of observed orbits in which Eq. (15.3) does not apply are those of binary pulsars and the Pioneer/Cassini anomalies. The standard model attempts to explain these orbits must be discarded because they are based on the geometrically incorrect Einstein Hilbert (EH) theory [1–12]. From Eq. (15.1):

$$\begin{aligned} -\epsilon = -c^2\left(\frac{d\tau}{d\lambda}\right)^2 = &-\left(1-\frac{r_S}{r}\right)c^2\left(\frac{dt}{d\lambda}\right)^2 \\ &+\left(1-\frac{r_S}{r}\right)^{-1}\left(\frac{dr}{d\lambda}\right)^2 + r^2\left(\frac{d\phi}{d\lambda}\right)^2 \end{aligned} \tag{15.4}$$

where ϵ is a constant of motion[13, 14]. From Killing vector analysis [11, 13, 14] the following are also constants of motion for all gravitational fields:

$$E_r = \left(1-\frac{r_S}{r}\right)\left(\frac{dt}{d\lambda}\right), \quad L_r = r^2\left(\frac{d\phi}{d\lambda}\right) \tag{15.5}$$

These constants of motion remain so under all conditions, including the conditions of a binary pulsar. Therefore the first type of ECE orbital equation is:

$$\frac{1}{2}\left(\frac{dr}{d\lambda}\right)^2 + V_r(r) = \frac{1}{2}E_r^2. \tag{15.6}$$

This equation has the units of energy if:

$$\lambda = \tau \tag{15.7}$$

where τ is the proper time [11, 13, 14] and if both sides of Eq. (15.6) are in S.I. units of joules. This is achieved by multiplying both sides by m to obtain:

$$\frac{1}{2}m\left(\frac{dr}{d\tau}\right)^2 + V = E = \frac{1}{2}mc^2E_r^2. \tag{15.8}$$

The potential energy of the system in joules is:

$$V = mV_r = \frac{1}{2}m\left(\epsilon - \epsilon\frac{r_S}{r} + \frac{L^2}{r^2} - \frac{r_SL^2}{r^3}\right)^2 \tag{15.9}$$

and the ECE orbital equation of type one, in S.I. units of joules is:

$$\frac{1}{2}m\left(\frac{dr}{d\tau}\right)^2 = E - V \tag{15.10}$$

with:

$$\epsilon = c^2. \tag{15.11}$$

Therefore the potential energy in joules is:

$$V = \frac{1}{2}m\left(1 - \frac{r_S}{r}\right)\left(c^2 + \frac{L}{r^2}\right) \tag{15.12}$$

with the constant of motion:

$$L = r^2\frac{d\phi}{d\tau}. \tag{15.13}$$

Various types of orbits can be found by integrating Eq. (15.10) numerically. In the standard model the radius r_S is always assumed to be:

$$r_S = \frac{2MG}{c^2} \tag{15.14}$$

and is incorrectly attributed [1–10] to Schwarzschild. This attribution is due to poor scholarship, Schwarzchild in 1916 produced a parameter α which was not identified with Eq. (15.14). The identification of α with the so called Schwarzschild radius is in fact arbitrary, as shown by Crothers [1–10]. The identification follows the data, and does not predict the data as claimed in the standard model. The observational fact is that there are orbits which do not obey Eq. (15.14). This is now understood [1–10] to be due to the fact that the EH equation is geometrically self-inconsistent for reasons carefully developed recently [1–10] in a series of proofs and arguments, and using computer algebra.

In a binary pulsar [11] for example the mean distance between the two component stars is decreasing per revolution. This decrease cannot be described by Eq.(15.14). In ECE theory the observed decrease per revolution is explained by using the fact that in general:

$$|r_S| = \frac{T}{R}(r, \theta, \phi). \tag{15.15}$$

A simple and well known [11] example of orbital theory is the limit of circular orbits:

$$\frac{\partial V}{\partial r} = 0. \tag{15.16}$$

From Eqs. (15.12) and (15.16):

$$r = \frac{1}{c^2 r_S}\left(L^2 \pm L\left(L^2 - 12c^2 r_S^2\right)^{\frac{1}{2}}\right). \tag{15.17}$$

In the Newtonian limit:

$$r_S \rightarrow 0 \tag{15.18}$$

and:

$$r \rightarrow \frac{L^2}{c^2 r_S}. \tag{15.19}$$

Therefore:

$$r \rightarrow \frac{L^2}{c^2}\frac{R}{T}. \tag{15.20}$$

In the Newtonian limit:

$$L \rightarrow rv \tag{15.21}$$

where v is the orbital velocity, so:

$$\frac{R}{T} \rightarrow \left(\frac{c}{v}\right)^2 \frac{1}{r}. \tag{15.22}$$

In the Newtonian limit it is known from observation that:

$$\frac{R}{T} = \frac{c^2}{2GM} \tag{15.23}$$

to an excellent approximation, so:

$$rv^2 = GM. \tag{15.24}$$

Therefore in the Earth to Sun system for example these Newtonian limits apply. Some numerical results and discussion on the self-consistency of this

analysis are given in Section 15.6. It is shown there that for a large enough T/R the orbital radius will decrease to zero, without assuming gravitational radiation. In a binary pulsar the orbit is elliptical, the masses of the two stars are about equal, and the ecliptic precesses a great deal every revolution. On top of this the distance between the two stars decreases. All these features are described by Eq. (15.10) and other types of ECE orbital equation, given the fact that T/R is in general a function of the spherical polar coordinates, and not a constant. This conclusion is also shown by the Pioneer/Cassini anomalies.

The binary pulsar is a two particle problem in dynamics, governed by:

$$\mathbf{r} = \mathbf{r}_1 - \mathbf{r}_2 \tag{15.25}$$

and

$$\mathbf{r}_1 = \frac{m_2}{m_1 + m_2}\mathbf{r}, \quad \mathbf{r}_2 = -\frac{m_1}{m_1 + m_2}\mathbf{r}, \tag{15.26}$$

where m_1 and m_2 are the masses of the two stars and where $\mathbf{r}_1$ and $\mathbf{r}_2$ are the distances between each star and the center of mass of the two star system. If the reduced mass is defined by:

$$\mu = \frac{m_1 m_2}{m_1 + m_2} \tag{15.27}$$

the lagrangian [13] is:

$$L = \frac{1}{2}\mu\left(\dot{r}^2 + r^2\dot{\phi}^2\right) - U(r) \tag{15.28}$$

in spherical polar coordinates. The following is a constant of motion:

$$l = \mu r^2\dot{\phi} \tag{15.29}$$

and this is Kepler's second law as is well known. The total energy of the system is constant:

$$E = T + U \tag{15.30}$$

and so the orbital law may be described by:

$$\phi(r) = \int \frac{l}{r^2}\left(2\mu\left(E - U - \frac{l^2}{2\mu r^2}\right)\right)^{-1/2} dr. \tag{15.31}$$

This law may be rewritten [13] in terms of the force:

$$F(r) = -\frac{\partial U}{\partial r} \tag{15.32}$$

as

$$\frac{d^2u}{dr^2} + u = -\frac{\mu}{l^2}\frac{1}{u^2}F(u) \tag{15.33}$$

where

$$u = \frac{1}{r}. \tag{15.34}$$

The centrifugal force is identified as [13]:

$$F_c = -\frac{\partial U_c}{\partial r} = \frac{l^2}{\mu r^3} = \mu r\dot{\phi}^2 \tag{15.35}$$

and the effective potential is:

$$V(r) = U(r) + \frac{l^2}{2\mu r^2}. \tag{15.36}$$

In Newtonian dynamics:

$$F(r) = -\frac{mMG}{r^2} \tag{15.37}$$

so:

$$U(r) = -\int F(r)dr = -\frac{mMG}{r}. \tag{15.38}$$

In Newtonian dynamics therefore:

$$V(r) = -\frac{mMG}{r} + \frac{l^2}{2\mu r^2}. \tag{15.39}$$

Eq. (15.33) may be integrated to give:

$$\frac{\alpha}{r} = 1 + \epsilon\cos(\theta) \tag{15.40}$$

where:

$$\alpha = \frac{l^2}{\mu k}, \quad \epsilon = \left(1 + \frac{2El^2}{\mu k^2}\right)^{\frac{1}{2}}, \tag{15.41}$$

and

$$k = mMG. \tag{15.42}$$

The quantity ϵ is known as the eccentricity of the orbit.

From these equation it is inferred that a Newtonian orbit is an exactly closed ellipse whose perihelion does not advance, i.e. in a Newtonian orbit:

$$\frac{d^2u}{d\phi^2} + u = \frac{Gm^2M}{l^2} \tag{15.43}$$

which is the orbit of a mass m attracted by a mass M through Newton's inverse square law. In the standard model the relativistic orbital equation becomes [13]:

$$\frac{d^2u}{d\phi^2} + u = \frac{Gm^2M}{l^2} + 3\frac{GM}{c^2}u^2 \tag{15.44}$$

i.e.

$$\frac{d^2u}{d\phi^2} + u = \frac{1}{\alpha} + \delta u^2 \tag{15.45}$$

using the notation:

$$\frac{1}{\alpha} = \frac{Gm^2M}{l^2}, \quad \delta = 3\frac{GM}{c^2}. \tag{15.46}$$

In ECE theory the orbital equation is Eq. (15.45) with:

$$GM = \frac{c^2}{2}\left|\frac{T}{R}\right| = \frac{c^2}{2}r_S. \tag{15.47}$$

Therefore orbits may also be described by numerically integrating the type two ECE orbital equation (15.45). The orbit of a binary pulsar is therefore described by finding u from Eq. (15.45) and using Eqs. (15.25) and (15.26) to find the individual orbits of the stars of the binary pulsar as a function of T/R. The latter is adjusted to fit the observed perihelion advance of 4^o per

revolution in the Hulse Taylor binary pulsar for example, and the observed decrease of 3.1 mm a revolution in the inter-star separation $\mathbf{r}_1 + \mathbf{r}_2$.

A third type of ECE orbital equation may be found by using:

$$\frac{dr}{d\phi} = \frac{dr}{d\tau}\frac{d\tau}{d\phi} = \frac{r^2}{L}\frac{dr}{d\tau} \tag{15.48}$$

so:

$$\frac{dr}{d\phi} = \frac{r^2}{L}\left(\frac{2}{m}(E-V)\right)^{\frac{1}{2}} \tag{15.49}$$

and:

$$\phi = \int \frac{L}{r^2}\left(\frac{2}{m}(E-V)\right)^{-\frac{1}{2}} dr. \tag{15.50}$$

This equation may be integrated numerically as a function of T/R to give such effects as light bending by gravitation as a function of T/R. So in general the light bending is not precisely twice the Newtonian value - this is an ECE prediction that can be looked for experimentally in for example the Joddrell Bank binary pulsar in which the two stars are each pulsars.

15.3 The Equivalence Principle

The inertial mass is that mass that determines the acceleration of a particle under the action of a given force [13]. The gravitational mass is that mass that determines the gravitational force between two particles. The two types of mass are the same within one part in 10^{12}. This is known as the equivalence principle. Thus:

$$F = mg = -\frac{mMG}{r^2} \tag{15.51}$$

and there exists an acceleration due to gravity that is independent of m. Thus two objects of different m fall to the surface of the Earth of mass M at the same time for a given r. This fact is usually attributed to Galileo but was known to the ancients, for example John Philoponus in the sixth century. The gravitational potential defines g as follows:

$$\mathbf{g} = -\boldsymbol{\nabla}\Phi \tag{15.52}$$

where:

$$\Phi = -\frac{GM}{r} \tag{15.53}$$

and the potential energy in joules is:

$$U = m\Phi. \tag{15.54}$$

In ECE the equivalence principle is a consequence of Cartan geometry, as might be expected. In ECE theory [1–10]:

$$g = Tc^2 \tag{15.55}$$

and:

$$\left|\frac{T}{R}\right| \rightarrow \frac{2MG}{c^2}. \tag{15.56}$$

Therefore Eq. (15.51) follows from Eqs. (15.55) and (15.56) if:

$$Tc^2 = \frac{c^2}{2}\left|\frac{T}{R}\right|\frac{1}{r^2} \tag{15.57}$$

i.e.:

$$R = \frac{1}{2r^2}. \tag{15.58}$$

Now use:

$$\left|\frac{T}{R}\right| = r_S = \frac{2MG}{c^2} \tag{15.59}$$

so from Eqs. (15.58) and (15.59):

$$|T| = \frac{r_S}{2r^2}. \tag{15.60}$$

Therefore the fundamental geometrical reason why m should be the same on both sides of Eq. (15.51) is that the curvature and torsion are given by Eqs. (15.58) and (15.60). The Pioneer/Cassini anomalies and the orbits of binary pulsars are due to the fact that r_S deviates from $2MG/c^2$, but the equivalence principle in ECE is always true, as for any theory of relativity.

15.4 Perturbation Theory of the Orbit of a Binary Pulsar System

In the simplest instance it is shown in this section that the main features of the orbit of a binary pulsar system can be explained with:

$$r_S = -\frac{T}{R} = \frac{2MG}{c^2} + \frac{a}{r} \tag{15.61}$$

where a is a parameter of the system. Therefore the potential energy of the binary pulsar is given by:

$$V = \frac{1}{2}m\left(1 - \frac{r_S}{r}\right)\left(c^2 + \frac{L^2}{r^2}\right) \tag{15.62}$$

with r_S defined as in Eq. (15.61). The latter produces an additional force of attraction:

$$\Delta F = -\frac{\partial \Delta V}{\partial r} = -\frac{2am}{r^3}\left(c^2 + \frac{2L^2}{r^2}\right). \tag{15.63}$$

It may be shown straightforwardly using Eq. (15.33) that this additional force of attraction results in a logarithmic spiral orbit of the type:

$$r = k^{\frac{1}{3}} \exp\left(\frac{\alpha}{3}\phi\right) \tag{15.64}$$

so that the complete orbit of the binary pulsar is a precessing ellipse superimposed on a logarithmic spiral. This result has been confirmed using computer simulation and is illustrated in Fig. (15.12). It can be seen that the observed decrease in orbital radius of 3.1 mm a revolution in a binary pulsar such as the Hulse Taylor binary pulsar can be reproduced by the simple assumption of Eq. (15.61). The ratio of torsion to curvature is assumed therefore to be of the form (15.61), in which a can be considered to be a small perturbation. In the solar system it is responsible for the Pioneer/Cassini anomalies, which is a small but finite extra gravitational attraction not given by the Einstein Hilbert theory. Therefore Eq. (15.61) gives a simple and consistent explanation of non EH orbits of all kinds without the assumption of gravitational radiation and by self consistently incorporating the Cartan torsion missing in the EH equation. The total potential of the binary pulsar system may be expressed as:

$$V = V_0 + \Delta V \tag{15.65}$$

where ΔV is an extra attractive potential due to Eq. (15.61). In an initially circular orbit:

$$\frac{\partial V_0}{\partial r} = 0 \tag{15.66}$$

and it is clear that the extra force of attraction due to ΔV will cause the orbit to spiral inwards on a logarithmic spiral trajectory of type (15.64). In the earth to sun system in the solar system the extra ΔV is very small, as can be seen from the Pioneer/Cassini anomaly, and the earth's orbit is essentially circular and non-relativistic. The advance of the perihelion for earth is very small per orbital revolution of one year. However in a binary pulsar the extra force of attraction causes the orbit to spiral inwards on a logarithmic spiral trajectory by an average of 3.1 mm a revolution. The orbit of the Hulse Taylor binary pulsar for example is very elliptical, and its perihelion advances by 4^o per revolution. The advance of the perihelion can be described by V_0 alone, but the decrease of the orbit needs for its explanation the additional ΔV. All binary pulsar systems currently catalogued can be described in this way, without the need to assume gravitational radiation.

One of the major discoveries of ECE theory [1–10] is that the EH equation is self inconsistent because of its neglect of torsion. Therefore all the physical predictions of the EH equation must be re-explained anew using ECE theory, in which the torsion is correctly incorporated. These include light deflection due to gravitation, perihelion advance, the orbits of binary pulsars, the Pioneer/Cassini anomalies, frame dragging, the Shapiro delay, and in general all the precision tests of relativity. Concepts such as Big Bang, dark matter theory, black hole theory, and so on must be rejected because they are based on a self-inconsistent geometry, Riemann geometry without torsion. Careful scholarship [1–10] has revealed that the Schwarzschild vacuum solutions of 1916 do not contain the parameter $2MG/c^2$, but a parameter α. Therefore α in Eq. (15.61) is modeled to give the experimentally observed orbits. In ECE theory the α parameter is recognized as the ratio of $-T/R$. The orbit of a binary pulsar has been described without assuming gravitational radiation. The latter is again a false concept based on the flawed EH equation, and gravitational radiation has never been directly observed. It is merely assumed to exist because EH theory cannot describe the decrease in the orbital radius of a binary pulsar. In ECE theory [1–10], gravitational radiation exists in principle from the ECE wave equation based on the tetrad postulate of Cartan geometry. However gravitational radiation is exceedingly difficult to observe, and has not yet been observed in a quarter century of effort. Therefore the exact solutions of the EH equation are obsolete because they are solutions of an inconsistent geometry. It has been shown in paper 93 onwards of ECE theory [1–10] that the Christoffel or symmetric connection is inconsistent with the Bianchi identiy as developed by Cartan. All exact solutions of the EH equation are based on the Christoffel symbol and so must be rejected. During

the course of development of ECE theory, new and self consistent methods of relativity theory have been devised.

In order to calculate non Einstein Hilbert orbits self-consistently the dependence of r_S on r and on the constants of motion is needed. Consider the potential energy of the relativistic Kepler problem using the notation of section 15.1:

$$V(r) = \frac{1}{2} m \left(1 - \frac{rs}{r}\right) \left(c^2 + \frac{L^2}{r^2}\right) \tag{15.67}$$

It is found that:

$$\frac{\partial V}{\partial r_S} = -\frac{m\left(\frac{L^2}{r^2} + c^2\right)}{2\,r} \tag{15.68}$$

The rate of change of V with r is:

$$\frac{\partial V}{\partial r} = \frac{m\,r_S}{2\,r^2}\left(\frac{L^2}{r^2} + c^2\right) - \frac{mL^2}{r^3}\left(1 - \frac{r_S}{r}\right) \tag{15.69}$$

Now use:

$$\frac{\partial V}{\partial r_S} = \frac{\partial V}{\partial r}\frac{\partial r}{\partial r_S} \tag{15.70}$$

to find:

$$\frac{\partial r_S}{\partial r} = -\frac{3\,r_S\,L^2 - 2\,r\,L^2 + c^2\,r^2\,r_S}{r\,(L^2 + c^2\,r^2)} \tag{15.71}$$

and

$$\frac{\partial r}{\partial r_S} = -\frac{r\,\left(L^2 + c^2\,r^2\right)}{3\,r_S\,L^2 - 2\,r\,L^2 + c^2\,r^2\,r_S} \tag{15.72}$$

Therefore by integration, the required dependence of r_S on r and L is found:

$$r_S = \int -\frac{3\,r_S\,L^2 - 2\,r\,L^2 + c^2\,r^2\,r_S}{r\,(L^2 + c^2\,r^2)} dr \tag{15.73}$$

Conversely, the dependence of r on r_S is found by the following integration:

$$r = \int -\frac{r\,\left(L^2 + c^2\,r^2\right)}{3\,r_S\,L^2 - 2\,r\,L^2 + c^2\,r^2\,r_S} dr_S. \tag{15.74}$$

The integral of Eq. (15.73) can be worked out analytically:

$$r_S(r) = \frac{\left(L^2 + c^2\, r^2\right)}{r^3}\left(2\, L^2\left(\frac{\log\left(L^2 + c^2\, r^2\right)}{2\, c^4} + \frac{L^2}{2\, c^4\, L^2 + 2\, c^6\, r^2}\right) + b\right) \tag{15.75}$$

while the integral of Eq. (15.74) is not solvable analytically. Solution (15.75) contains the integration constant b which leads to a threefold classification of the results:

$$r_S \rightarrow \begin{cases} +\infty \\ -\infty \\ 0 \end{cases} \quad \text{for } r \rightarrow 0.$$

Examples of the first two classes are graphed in Section 5.2. Self-consistency of the perturbation model is shown there by deriving an expression for the perturbation parameter a which is compatible with the r dependence of r_S.

In Section 15.6 a review of known binary pulsar systems is given from a recent observational survey. These orbits are all likely to be non EH orbits and in future work they will be catalogued using Eq. (15.61), so that each can be assigned an a parameter. Furthermore, orbits of all kinds can be described by Eq. (15.61), for example the equation shows that the earth's orbit will very slowly spiral into the sun due to the non EH attractive force discovered by both the Pioneer and Cassini spacecraft as they escape the solar system. This is equivalent to a g of order $10^{-12}\mathrm{ms}^{-2}$. So Eq. (15.61) is a suggestion for a self consistent cosmology, one that explains all orbits without gravitational radiation, and one which correctly takes account of the Cartan torsion in relativity theory.

15.5 Graphical Results and Discussion

15.5.1 Schwarzschild Radius and Potential

The results of the analytical and numerical calcualtions are presented in this section. First the effect of a variable Schwarzschild radius r_S was studied. A parametric form

$$r_S = \gamma\, r_{S0} \tag{15.76}$$

was used where r_{S0} is the value from standard theory:

$$r_{S0} = \frac{2GM}{c^2} \tag{15.77}$$

Table 15.1 Simulation parameters (in SI units).

	Earth/Sun	Hulse-Taylor
m_1	$5.9742 \cdot 10^{24}$kg	$2.86629 \cdot 10^{30}$kg
m_2	$1.9891 \cdot 10^{30}$kg	$2.75888 \cdot 10^{30}$kg
r_1	$1.4960 \cdot 10^{11}$m	$3.15357 \cdot 10^{9}$m
L	$4.4580 \cdot 10^{15}$m^2/s	$3.4 \cdot 10^{14}$m^2/s

and γ is an adjustable parameter. In the Newtonian limit the orbital radius r depends inversely linear on r_S, see Eq. (15.19). This is graphed in Fig. (15.1) for the earth radius in the solar system. For $\gamma = 1$ it takes the standard value of about $1.5 \cdot 10^{11}$m but falls hyperbolically to zero for a largely increased r_S.

In Fig. (15.2) the Newtonian limit of Eq. (15.19) is compared with the relativistic case described by Eq. (15.17). With the parameters of the solar system (Table (15.1)) both approaches lead to indistinguishable values with exception of a very large r_S where the relativistic curve drops to a vertical tangent. Beyond this range, the square root expression of Eq. (15.17) is imaginary. It can be seen that both equations are self-consistent because they result in the same curve over a wide range of r_S.

Next the relativistic potential of Eq. (15.12) is described and graphed by some examples. In the Newtonian case the term proportional to $1/r^3$ is absent, i.e. r_S is effectively set to zero for this part. From Fig. (15.3) the principle difference between the Newtonian and relativistic case can be seen (the term $1/2\,mc^2$ has been omitted). In the Newtonian case the potential goes to plus inifinity for small radii, while it falls to minus inifinity in the relativistic case. This does not change significantly if parameters are altered. For example in Fig. (15.4) we have increased the mass of the earth artificially to that of the sun. Theoretically the relativistic curve could have a local maximum, but this does not show up in the parameter range considered here. The behaviour of the Newtonian potential changes if the angular momentum of the earth would be considerably lower as indicated in Fig. (15.5). However, all this would happen inside the radius of the sun and therefore is beyond reality.

The change in the potential for a varying r_S can be studied from Fig. (15.6). For increasing r_S, there is no visible change in the Newtonian potential,

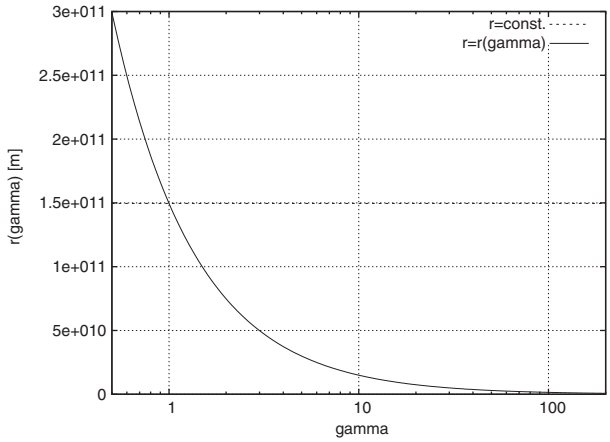

Fig. 15.1. Orbital radius r of Earth in dependence of variable Schwarzschild radius $r_S = \gamma \cdot r_{S0}$.

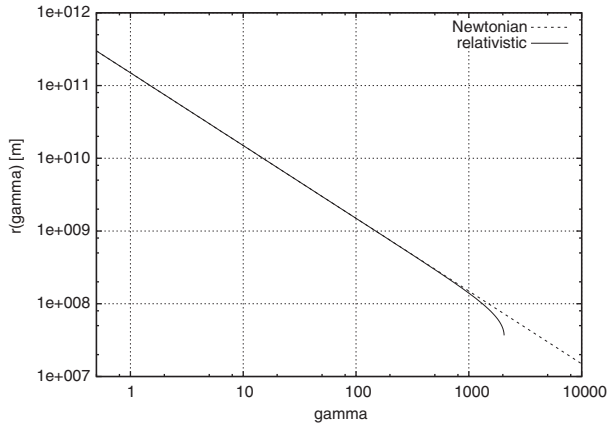

Fig. 15.2. Orbital radius of Earth in dependence of variable Schwarzschild in Newtonian and relativistic limit.

but a tendency to an earlier dropping in the relativistic case. The behaviour of the Newtonian potential is different for a reduced angular momentum (Fig. (15.7)). Increasing the Schwarzschild radius leads to a significant lowering of the potential near to the center.

15.5.2 Self-Consistency of Schwarzschild Radius Calculations

According to the results of section 15.4, r_S can be obtained as a function of the radius by integration (Eqs. 15.73, 15.75). The solution (15.75) contains the

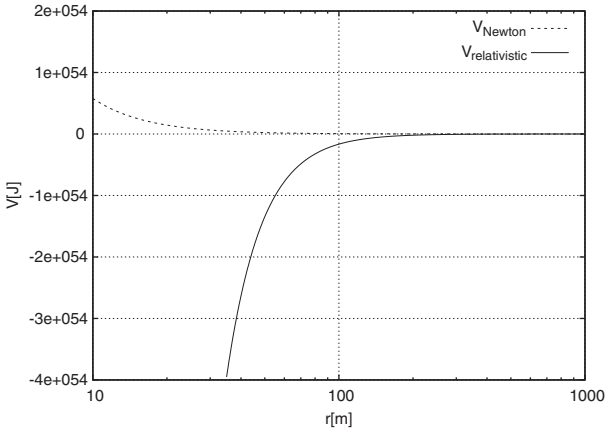

Fig. 15.3. Potential of Sun for Earth, r_S = 2954 km, m = m(Earth), L = L(Earth).

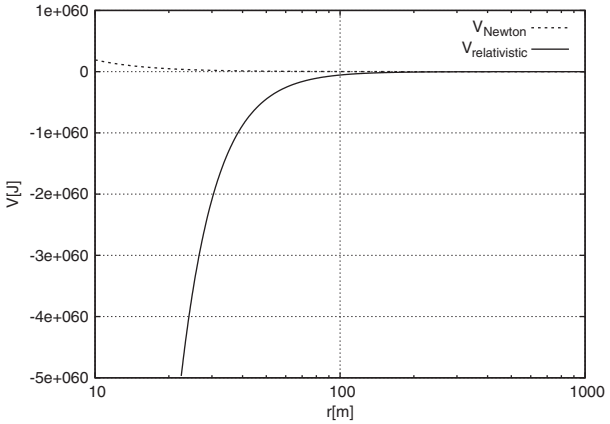

Fig. 15.4. Potential of Sun for enhanced earth mass, r_S = 2954 km, m = m(Sun), L = L(Earth).

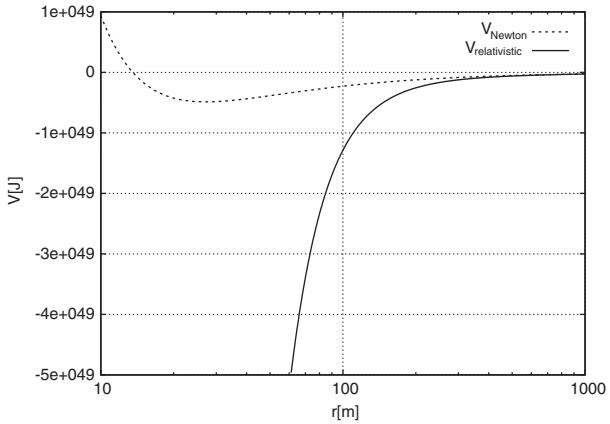

Fig. 15.5. Potential of Sun for enhanced earth mass, $r_S = 2954$ km, m=m(Sun), lowered angular momentum: $L = 6 \cdot 10^{10}\mathrm{m}^2/\mathrm{s}$ (reduced).

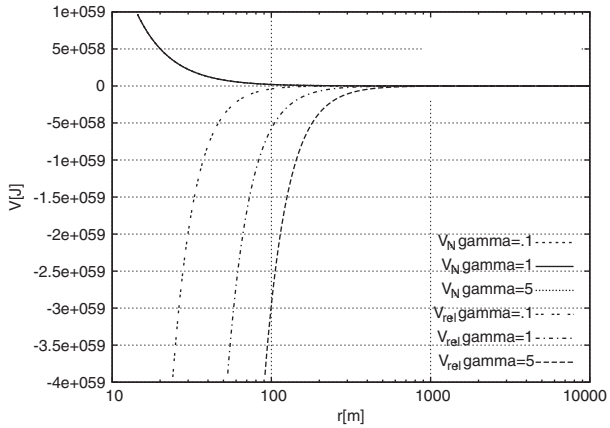

Fig. 15.6. Dependence of Potential of Sun from $|T/R|$, for $|T/R| = \gamma \cdot r_S$ with $r_S = 2954$ km, m=m(Sun), L = L(Earth).

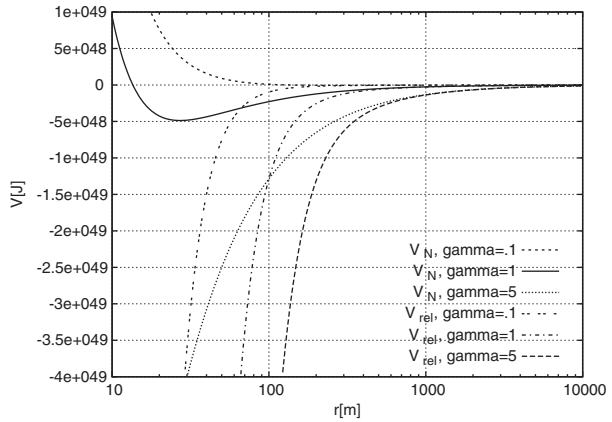

Fig. 15.7. Dependence of Potential of Sun from $|T/R|$, for $|T/R| = \gamma \cdot r_S$ with $r_S = 2954$ km, m = m(Sun), L = $6 \cdot 10^{10}$m^2/s (reduced).

integration constant b which leads to a threefold classification of the results: $r_S \to +\infty, -\infty, 0$. Examples of the first two classes are graphed in Fig. (15.8). The third class of solutions is defined by $r_S(r)$ hitting the coordinate origin:

$$r_S(0) = 0.$$

This is the type of solution which is physical because it has the right asymptotic behaviour

$$r_S \to 0 \quad \text{for} \quad r \to 0.$$

This is a bound solution while the other two classes are unbound solutions. Setting

$$r_S(r) = 0 \tag{15.78}$$

defines the constant b for which this condition is met, in dependence of r:

$$b = -\frac{\left(L^4 + c^2\, r^2\, L^2\right)\, \log\left(L^2 + c^2\, r^2\right) + L^4}{c^4\, L^2 + c^6\, r^2}. \tag{15.79}$$

We obtain the desired value of the constant by setting $r = 0$:

$$b = -\frac{L^2\ (2\ \log(L) + 1)}{c^4}. \tag{15.80}$$

This expression depends sensitively on the constant of motion L. By construction, r_S should have the known value of 2954 m for the earth orbit. For $L(Earth)$ we obtain the upper curve in Fig. (15.9) which does not meet this condition properly. Therefore we have adopted the value of L to $L = 1.42 \cdot 10^{15}\mathrm{m}^2/\mathrm{s}$ so that the curve goes through the point

$$r_S(1.49 \cdot 10^{11}\mathrm{m}) \approx r_{S0} = 2954\,\mathrm{m}.$$

This leads to the lower curve in Fig. (15.9). The numerical analysis shows that the formula for r_S depends sensitively on the value of b. Since we are operating with very large numbers here (up to 10^{60}) the numerical stability is not very high even in evaluating analytical formulae. This point has to be further investigated in subsequent work, perhaps by switching to astronomical units. Here we restrict to showing up the basic properties of a variable $r_S(r)$.

To circumvent this problem we try another approach for model 3. The integration constant b is defined now by the condition

$$r_S(r_{Earth}) = r_{S0}.$$

This gives the result graphed in Fig. (15.10). r_S takes a maximum at the earth radius. This approach is not sufficient since r_S takes negative values for small r.

As a last point in this subsection we inspect the behaviour of the perturbation model Eq. (15.61) in section 15.4. For reasons of self-consistency, the parameter a must be a function of r so that both models can coincide. Therefore we have, with Eq. (15.75):

$$r_{S0} + \frac{a}{r} = \frac{\left(L^2 + c^2\,r^2\right)}{r^3}\left(2\,L^2\left(\frac{\log\left(L^2 + c^2\,r^2\right)}{2\,c^4} + \frac{L^2}{2\,c^4\,L^2 + 2\,c^6\,r^2}\right) + b\right). \tag{15.81}$$

and after resolving for a:

$$a = \frac{\left(L^4 + c^2\,r^2\,L^2\right)\log\left(L^2 + c^2\,r^2\right) + L^4 + b\,c^4\,L^2 - c^4\,r^3\,r_{s0} + b\,c^6\,r^2}{c^4\,r^2}. \tag{15.82}$$

Using the three models of Figs. (15.9) and (15.10) we obtain three distinct values for b and therefore three different solutions for Eq. (15.81), graphed in Fig. (15.11). Models 1 and 3 have a maximum at the earth orbit. Models 2 and 3 lead to $a = 0$ at the earth orbit by construction. It can be seen from the graphs that this condition is fulfilled. Model 3 gives negative values for a and therefore seems to be the worst one. Model 2 is the only model with

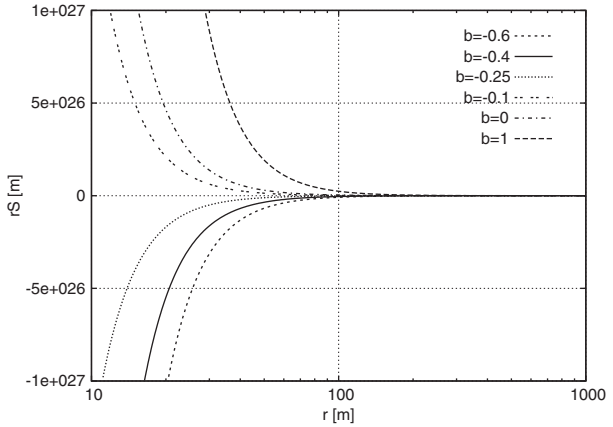

Fig. 15.8. Dependence of Potential of Sun from $|T/R|$, for $|T/R| = \gamma \cdot r_S$ with $r_S = 2954$ km, m = m(Sun), L $= 6 \cdot 10^{10}$m^2/s (reduced).

increasing, non-negative a for $r < r(Earth)$ and seems to be most compatible with the perturbation model.

We can conclude that the self-consistent calculation of r_S is in principle compatible with the perturbation model, but it is quite difficult to find the "physical" integration constant because the results depend sensitively on it.

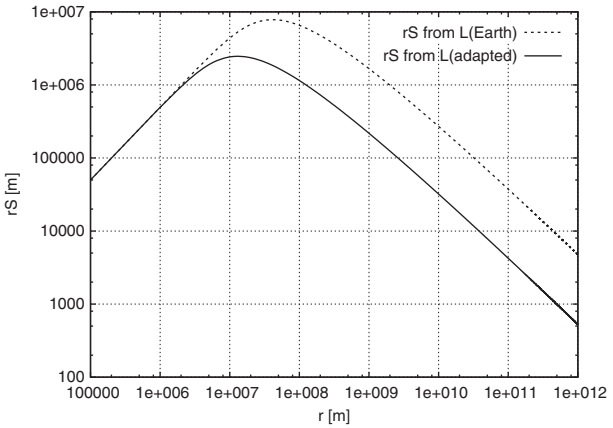

Fig. 15.9. Solutions of third type for $r_S(r)$ going through the coordinate origin, for original L(Earth) and adapted L.

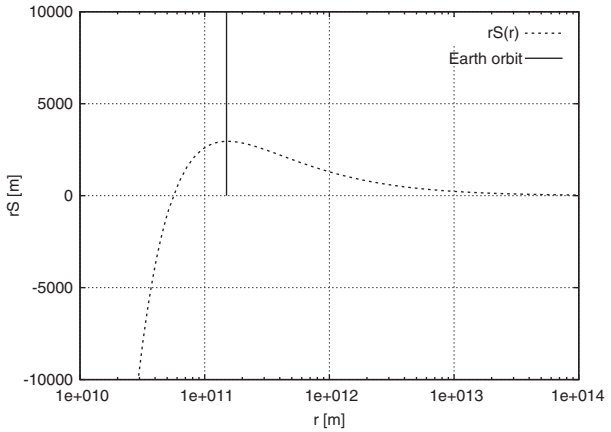

Fig. 15.10. $r_S(r)$ for integration constant b defined from condition $r_S(r_{Earth}) = r_{S0}$.

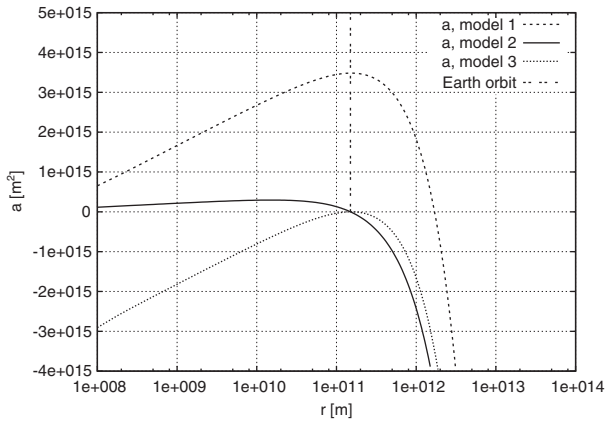

Fig. 15.11. Self-consistent parameter a for perturbation term of r_S, for three models.

15.5.3 Simulations of Orbits

The computation of orbits is based on Eqs. (15.44–15.46). Since these are not soluble analytically, a simulation program was written on base of the Runge-Kutta algorithm. With this method, coupled ordinary differential equations of first order can be solved in 4th order precision. The set of equations is

$$\frac{du}{d\phi} = w, \tag{15.83}$$

$$\frac{dw}{d\phi} = \frac{1}{\alpha} + \delta u^2 - u \tag{15.84}$$

with

$$\frac{1}{\alpha} = \frac{G\mu^2 m_2}{l^2} = \frac{\mu^2}{l^2}\frac{c^2}{2} r_S, \tag{15.85}$$

$$\delta = \frac{3Gm_2}{c^2} = \frac{3}{2} r_S^2, \tag{15.86}$$

μ being the reduced mass, $l = L\mu^2$ the angular momentum and w an auxiliary variable (inverse radial velocity). Without the δu^2 term, the orbits $r(\phi) = 1/u(\phi)$ have the form of ellipses. The effect of the relativistic δu^2 is to prevent the elliptic orbits from being closed curves, there is an advance of the perihelion per revolution. With a constant r_S the minimum and maximum radius would not change, but they do if r_S depends on the radius. Both effects (relativistic term and a variable r_S) are inlcuded in the results shown in Fig. (15.12) where they can be observed nicely. The shrinking of radius is made more visisble in Fig. (15.13). One sees that the outer radius shrinks faster than the inner radius, thus stabilizing the orbit for a long time. Correspondingly, the inverse orbital velocities, described by the function $w(\phi)$, shrink in the same way (Fig. (15.14)) so that the total energy remains constant.

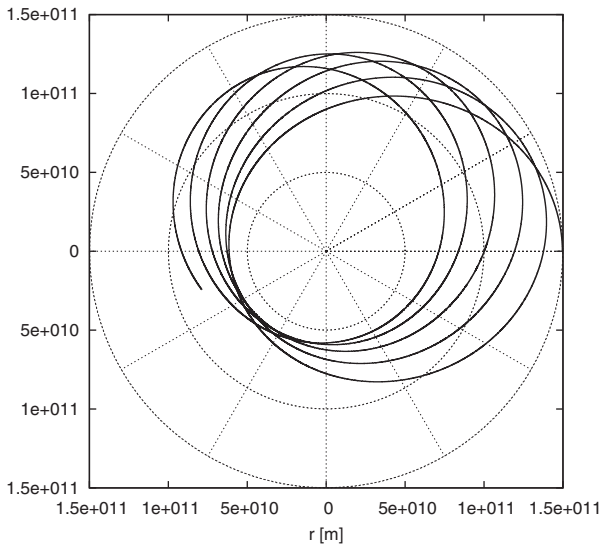

Fig. 15.12. Orbit $r(\phi)$ for a relativistic potential with Schwarzschild radius perturbation a/r.

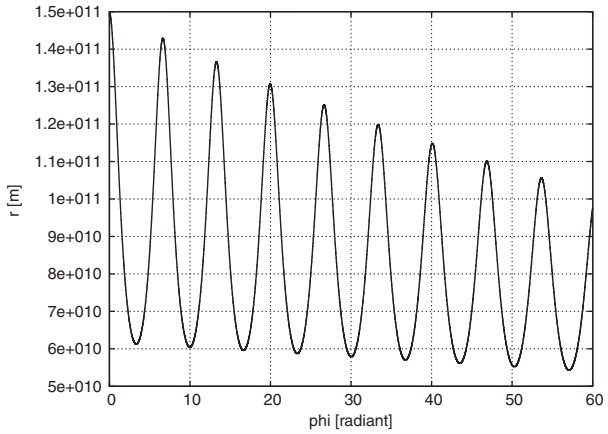

Fig. 15.13. Angular dependence of orbital radius r of Fig. 15.12.

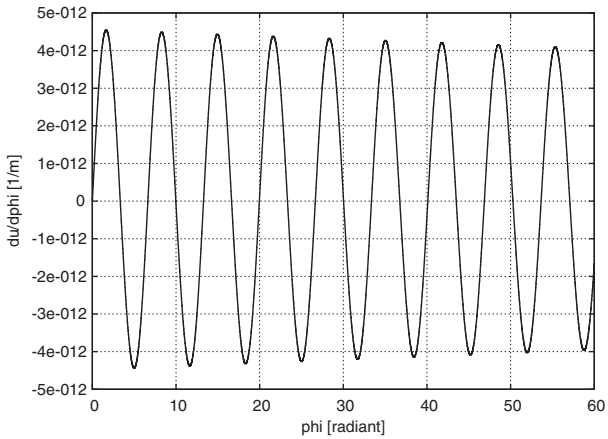

Fig. 15.14. Angular dependence of inverse velocity w of Fig. 15.12.

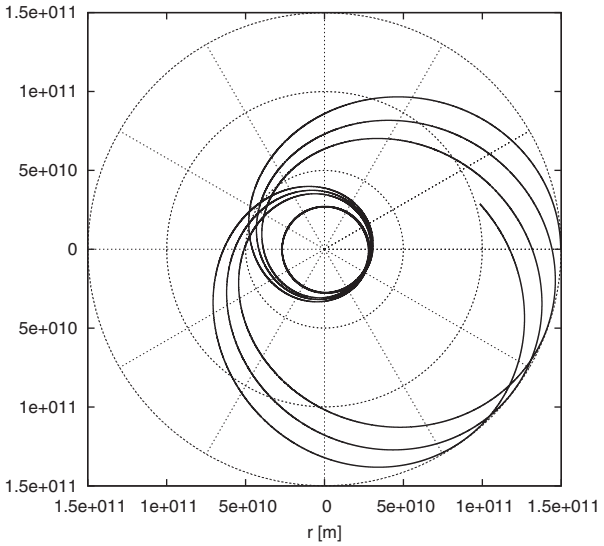

Fig. 15.15. Orbit $r(\phi)$ for a relativistic potential with Schwarzschild radius dependence according to model 2.

For the more complicated models of $r_S(r)$ other types of orbits are to be expected. Applying the model of Fig. (15.9), there is a maximum of $r_S(r)$ which leads to two stable orbital radii and the mass body oscillates between both (Fig. (15.15)). This is in accordance with orbits of periodic central fields as described in [13].

15.6 Pulsars and Double Star Systems

15.6.1 History of Discovery

Sir Arthur Eddington famously led an expedition to observe the total eclipse of the Sun in 1919 to see if light grazing the Sun was deflected by gravity according to the Einstein-Hilbert equation of general relativity. The conclusion that the Einstein-Hilbert equation described the bending of light better that Newtons work, led to Einstein becoming the world's first global superstar scientist and introduced the public to Einstein's concept of gravity as the curvature of space by massive objects. Here, mass tells space how to bend and space tells masses how to move!

Looking further into space than the Sun astronomers have sought to locate objects in the space with much greater gravitational fields than the Sun in order to improve the accuracy of the Edddington experiment, which was carried out close to the limit of experimental accuracy. The objects which are frequently studied for this purpose are white dwarfs, neutron stars and

pulsars. The intense beam of light from pulsars make them particularly suited to testing out general relativity.

The first pulsar to be discovered was by the postgraduate student Jocelyn Bell Burnell at Cambridge University in the nineteen sixties. Pulsars are stars that have lived their lives, gone supernova and collaped to produce neutron stars which have most of the mass of the original star, but concentrated into a much smaller volume. The concentration of the mass increases the gravity of the collapsed star in its neighborhood and this leads to a much greater curving of space, as predicted by Einstein's theory of general relativity.

In 1974 the first binary double star to have a pulsar as one of the components was discovered by Hulse and Taylor 21,000 light years away in the constellation of Hercules using the Arecibo radio antenna. The binary pulsar is in orbit with another star, with both components having a mass 1.4 times that of the Sun and the binary nature of the pulsar being given away by the 7.75 hour periodic variations in the arrival times of the radio pulses due to the pulsar approaching and receeding, which corresponds with the time taken for the system to complete one orbit. The Hulse Taylor binary pulsar was widely studied as a test bed for general relativity and gave its discoverers the 1993 Nobel Prize for Physics. About one hundred double pulsars have been found so far, giving researchers a range of orbits to and masses to study. However, the disovery of a binary double star in which both components were pulsars and in which both pulsar beams were reaching Erth would be not just an amazing stoke of luck, but would also be the system of choice to use to study general relativity!

The first and only double pulsar system ever found is called PSR J0737-3039A, B and was discovered by the Jodrell Bank radio-observatory in Manchester in January 2004.

The PSR prefix stands for pulsar and the letters A and B refer to the two component pulsars that are trapped by the immense gravitational field into mutually orbiting one another as a binary double star. Binary double stars are common, but for one of the components of a double star to be a pulsar is rare, because pulsars are comparatively rare and for both components to be a pulsar is a godsend, one of the greatest discoveries in all of science.

15.6.2 Numerical Results for the Hulse Taylor Double Star System

The doubls star system was simulated as described in section 5.3. The orbit of both masses is depicted in Fig. (15.16). Both stars move on ellipses with a common focal point. The relations between the geometric parameters are

$$e = \sqrt{a^2 - b^2}, \tag{15.87}$$

$$\epsilon = \frac{e}{a} = \frac{\sqrt{a^2 - b^2}}{a}, \tag{15.88}$$

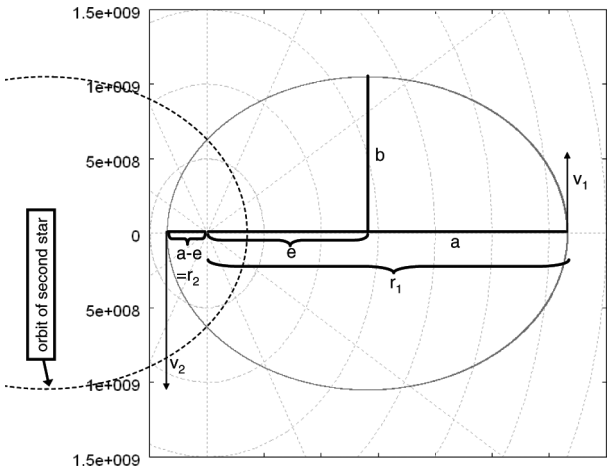

Fig. 15.16. Hulse-Taylor pulsar double star system, orbit and parameters.

$$b = a\sqrt{1-\epsilon^2} \tag{15.89}$$

with excentricity ϵ. The angular momentum parameter L can be determined in a simple way at the aphelion and perihelion points where the orbital velocity v is perpendicular to the radius, i.e. its radial component vanishes:

$$L = (a+e)v_1 = (a-e)v_2. \tag{15.90}$$

The kinetic, potential and total energy can be derived from the computed variables u and w in the following way. For w we have

$$w = \frac{du}{d\phi} = \frac{du}{dr}\frac{dr}{d\phi} = -\frac{1}{r^2}\frac{dr}{d\phi} \tag{15.91}$$

or

$$\frac{dr}{d\phi} = -wr^2. \tag{15.92}$$

With this equation we have

$$\dot{r} = \frac{dr}{d\phi}\frac{l}{\mu r^2} = -\frac{wl}{\mu}. \tag{15.93}$$

Therefore the kinetic energy becomes

$$T = \frac{1}{2}\left(\mu\dot{r}^2 + \frac{l^2}{\mu r^2}\right) = \frac{l^2}{2\mu}\left(w^2+u^2\right). \tag{15.94}$$

Note that the centrifugal potential belongs to the kinetic energy. The potential energy is

$$U = \frac{1}{2}\mu\left(c^2 - \frac{r_S}{r}c^2 - r_S\frac{l^2}{\mu^2 r^3}\right) \tag{15.95}$$

and the total energy

$$E_{tot} = T + U. \tag{15.96}$$

These energies have been plotted in Fig. (15.17). It can be seen that the total energy is conserved throughout the orbit. Kinetic and potential energy are highest in the region of maximal closeness of the stars, i.e. in the perihelion.

The relativistic part of the potential is compared to the Newtonian part (see Eq. (15.12)) in Fig. (15.18). The distance of the stars, even being closer than the sun-earth system, is large enough to make the relativistic effects small compared to the Newtonian part of the potential. It can nicely be seen that relativistic effects are highest in the perihelion, while they tend to zero in the aphelion.

Finally the effect of the parameter a of the perturbation model of the Schwarzschild radius is shown (Fig. (15.19)). The decrease in radius per revolution, Δr, is graphed against a. Obviously the dependence is linear over a range of several orders of magnitude. The physical value of Δr is some millimeters per revolution, so a has to be chosen in the range of $10^{-4}\mathrm{m}^2$. The

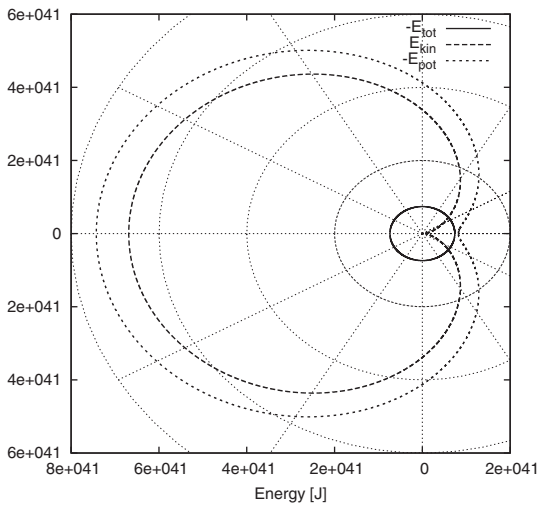

Fig. 15.17. Hulse-Taylor pulsar double star system, energy.

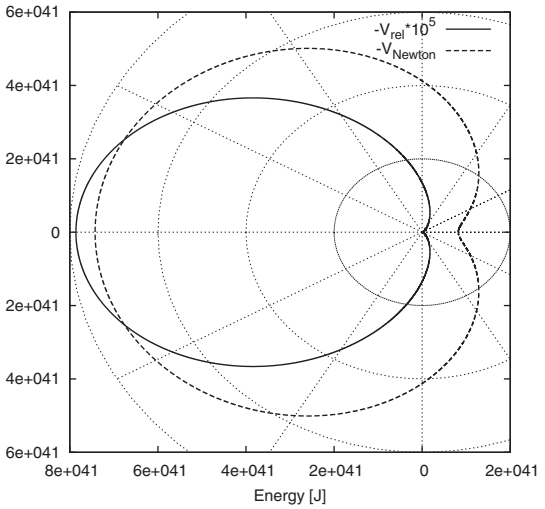

Fig. 15.18. Hulse-Taylor pulsar double star system, relativistic effects (enhanced by 10^5).

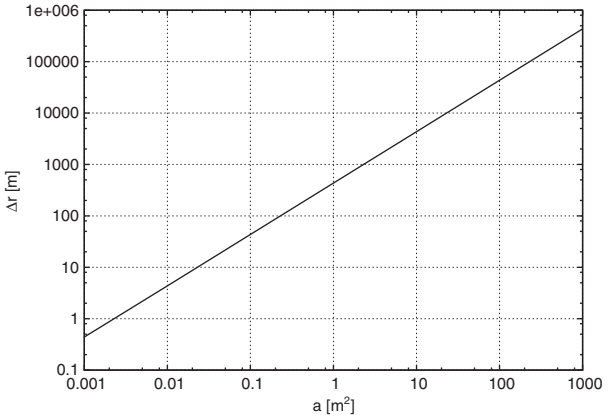

Fig. 15.19. Hulse-Taylor pulsar double star system, radius change per revolution Δr in dependence of perturbation a.

exact value is beyond the precision of the calculation. Although the Runge-Kutta scheme is precise to the order 4, the computed orbit was not stable enough to account for such small differences compared to the ellipse radius. We leave the exact determination of a to later numerical studies.

References

[1] M. W. Evans, "Generally Covariant Unified Field Theory" (Abramis, Suffolk, 2005 onwards), in five volumes to date (see also www.aias.us).

[2] K. Pendergast, "Crystal Spheres", preprint on www.aias.us.

[3] L. Felker, "The Evans Equations of Unified Field Theory" (Abramis, 2007).

[4] M. W. Evans, Omnia Opera Section of www.aias.us (1992 to present).

[5] M. W. Evans, (ed.), Adv. Chem. Phys., vol. 119 (2001), ibid., M. W. Evans and S. Kielich, vol. 85 (1992, 1993, 1997).

[6] M. W. Evans and L. B. Crowell, "Classical and Quantum Electrodynamics and the B(3) Field" (World Scientific, 2001).

[7] M. W. Evans and J.-P. Vigier, "The Enigmatic Photon" (Kluwer, 1994 to 2002), in five volumes.

[8] M. W. Evans and H. Eckardt, Physica B, 400, 175 (2007).

[9] M. W. Evans, Physica B, 403, 517 (2008).

[10] M. W. Evans, Acta Physica Polonica, B, 38, 2211 (2007).

[11] S. P. Carroll, "Spacetime and Geometry: an Introduction to General Relativity" (Addison Wesley, New York, 2004, and online 1997 notes).

[12] These are reviewed on www.telesio-galilei.com.

[13] J. B. Marion and S. T. Thornton, "Classical Dynamics" (HBC, New York, 1988, 3rd. ed.).

[14] R. M. Wald, "General Relativity" (Univ. Chicago Press, 1984).